32nd URSI GASS, Montreal, 19-26 August 2017

Aperture Field Transformation in Resonant Cavity Antennas by Transverse Permittivity Gradient Superstrates

Raheel M. Hashmi* (1) and Karu P. Esselle(2)
Department of Engineering, Faculty of Science and Engineering
Macquarie University, NSW 2109, Australia

Abstract

Single-feed resonant cavity antennas (RCAs) with transverse permittivity gradient (TPG) superstrates exhibit very wideband directivity enhancement. In this paper, we study the transformation of transverse electric field that is achieved by the TPG superstrate. This provides physical insight into the operating principle of such RCAs. Two fictitious apertures are used to record and compare the phase of the field within the cavity of the RCA as well as above its TPG superstrate. It is found that the TPG superstrate significantly reduces the phase variation of the aperture field over most of the operating bandwidth, thus resulting in wideband directive characteristics. Numerical results as well as measurements are presented showing wideband antenna performance with a peak directivity exceeding 16 dBi.

1. Introduction

Resonant cavity antennas (RCAs) are superstrate-based antennas that serve as a simple alternative to achieve highly directive characteristics [1-3]. RCAs are able to achieve high directivity with only a single source as opposed to other complex approaches such as antenna arrays [4]. Recently, a new class of compact RCAs has been proposed, which uses single-layer, all-dielectric superstrates and produces very wide directivity bandwidths [5], [6]. The superstrates in these RCAs have a transverse permittivity gradient (TPG) rather than having a constant permittivity along the superstrate, as used to be the case previously. The presence of this TPG allows these RCAs to achieve remarkably wide 3dB bandwidths (>50%) alongside good broadside directivity (>15dBi).

A common RCA has an air-filled cavity that is formed between a partially reflecting superstrate (PRS) and a ground plane. The cavity is excited by a simple feed antenna such as a slot, and the waves excited within this cavity create a directive beam transverse to the PRS (i.e., towards broadside) as a result of multiple reflections between the ground plane and the PRS. Conventionally, RCAs have exhibited narrow directivity bandwidths (often <5%). Non-uniformity of phase in the aperture field has often been identified as a reason for the limited directivity bandwidth of RCAs. In this paper, we study the transformation of transverse electric field by the TPG superstrates to understand the underlying cause of wide directivity bandwidths exhibited by RCAs with TPG superstrates.

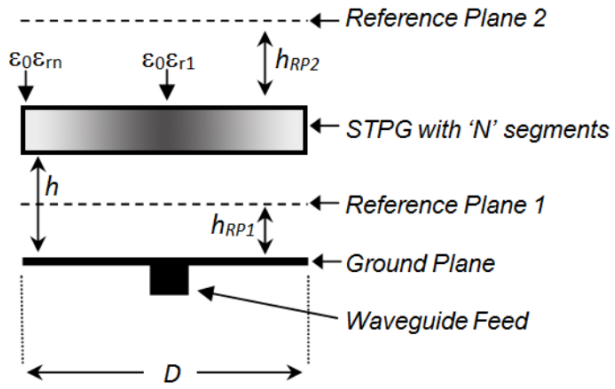

Figure 1. An RCA with a typical all-dielectric superstrate having transverse permittivity gradient. Reference plane 1 (RP1) and reference plane 2 (RP2) are also shown.

2. Antenna Configuration and Observation Planes

The basic configuration of an RCA with a TPG superstrate is shown in Fig 1. The superstrate is a single-layer dielectric disc with its relative permittivity decreasing gradually from $\varepsilon_1 = \varepsilon_{r0}\varepsilon_1$ to $\varepsilon_1 = \varepsilon_0\varepsilon_{rn}$. This decrease is approximated by segmenting the superstrate disc into nine radial segments (N=9) where the dielectric constants $\{\varepsilon_1, \varepsilon_{2,\ldots,} \varepsilon_9\} = \{10, 9, ..., 2\}$. The width of the first segment is $w_1 = 8$mm, and the widths of the remaining segments $\{w_2, ..., w_9\} = 2.875$mm.

The superstrate is placed at height $h = 13.5$mm above a ground plane, and the diameter of the ground plane and the superstrate is D = 54mm. All segments in the superstrate have equal thickness which is fixed to 4.25mm. Two reference planes are shown in Fig. 1 as RP1 and RP2, which are used to compute the transverse electric field within the cavity and above the superstrate, respectively. The reference planes are horizontally symmetric and are placed at heights $h_{RP1} = 6.75$mm, and $h_{RP2} = 3.375$mm, respectively. A linearly polarized waveguide-fed slot was cut in the center of the ground

plane to feed the RCA. Numerical simulations for this study are carried out in CST Microwave Studio using the time-domain solver.

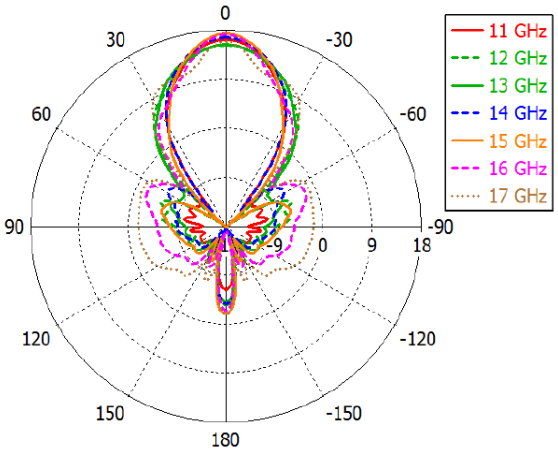

Figure 2. Directivity patterns of the RCA at 7 frequencies within the directivity bandwidth.

3. Field Transformation and Directivity Enhancement

Fig. 2 shows the computed directivity patterns of the RCA at seven frequencies within the 3dB directivity bandwidth (10.48–17.67 GHz). A peak directivity of 17.3dBi at 15 GHz is predicted and the side lobe levels are below −15 dB over most of the directivity bandwidth. To understand the cause of such wideband directivity enhancement, we evaluate the phase of the transverse electric field in this RCA. Fig. 3 shows the normalized phase distributions along the diameter of the RCA at four frequencies within the directivity bandwidth. It can be seen that the phase above the cavity (i.e. at RP2) is significantly uniform than the phase within the cavity (RP1). From the 10.5 GHz up to 16 GHz, the phase change ($\Delta\Phi$) remains <90°. This creates a uniform aperture and thus, results in a gradual increase of directivity from 14.4 dBi at 10.5 GHz to 17.4 dBi at 15.5 GHz. After 16 GHz, $\Delta\Phi$ begins to increase and exceeds 90°, reaching up to 150° at 17 GHz, which causes the directivity to decrease to 14.4 dBi (-3dB level) at 17.7 GHz. Minor fluctuations in the center region of phase distributions corresponding to RP1 can be observed in Fig. 2 (a). These fluctuations are due to feed antenna effects as the field in the RCA cavity has wave components that propagate in transverse directions, contrary to a pure in-phase standing wave which exists in an ideal resonant cavity.

The Huygens-Fresnel principle states that the secondary wavefronts radiated from two arbitrary points in RP2 behave as secondary radiating sources. If their individual field strengths is α and the phase difference between them is $\Delta\Phi$, then each secondary source creates a power density S towards broadside, which is proportional to $|\alpha|^2$. When $\Delta\Phi \rightarrow 0^o$, then $S = |\alpha+\alpha|^2 = 4\alpha^2$ whereas when $\Delta\Phi \rightarrow 90^o$, this drops to half, i.e., $S = |\alpha+j\alpha|^2 = 2\alpha^2$. As $\Delta\Phi \rightarrow 180^o$, the sources add up destructively, deteriorating the aperture field and thus, decreasing the directivity of the RCA.

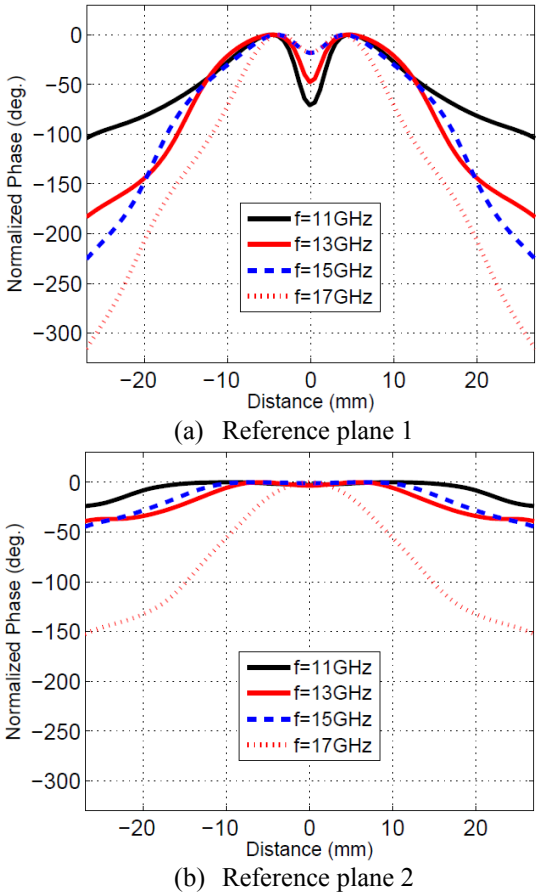

Figure 3. Aperture field distribution of the computed for the RCA (a) within the cavity of RCA, (b) at the reference plane above the TPG superstrate.

4. Experimental Results

A prototype antenna was designed using CST time-domain solver to validation of the proposed concept. Commercially available dielectric materials were used to construct a circular superstrate with radius R = 21mm for the fabricated prototype. To simplify the fabrication process, extensive simulations were conducted to quantify the compromise in selecting the minimum number of steps in the superstrate, and the best achievable wideband, directive performance. Considering this study, 3-steps were used in the superstrate, with $\varepsilon_1 = 10.2$, $\varepsilon_2 = 6.15$, and $\varepsilon_3 = 3.27$. All sections were set to the same, commercially available thickness of 4.4 mm. To feed the antenna, a rectangular slot with dimensions 12mm × 7.5mm was cut in the middle of the ground plane, and fed with WR-75 waveguide-to-coax adaptor.

The performance of this prototype antenna was measured in NSI-700S-50 spherical near-field chamber. The prototype demonstrated a peak directivity of 16.4 dBi

with a 3dB directivity bandwidth extending from 10GHz to 17.2 GHz i.e., 52.9 %. Input impedance matching measured using Agilent PNA-X N5242A vector network analyser is shown in Fig. 4. It can be seen that $|S_{11}|$ remains below –10 dB over most of the directivity bandwidth with a minor deterioration in $|S_{11}|$, reaching a maximum value of –8.2 dB around 11-12 GHz. However, it only reduces the gain of the ERA by approximately 1dB at this frequency and the gain bandwidth of the antenna was found to extend from 10 GHz – 17.45 GHz. A sharp spike can be observed at 17.55 GHz above the upper end of the bandwidth in Fig. 4. This spike is attributed to the SMA transition in the commercial WR-75 waveguide adaptor, which was not considered in the simulation model.

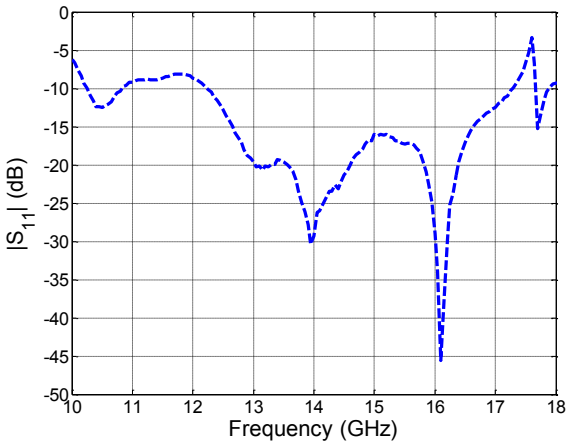

Figure 4. Measured input reflection coefficient of the antenna prototype.

5. Conclusions

Aperture field transformation in single-feed resonant cavity antennas (RCAs) with transverse permittivity gradient (TPG) superstrates was studied to evaluate the cause of their wideband directive characteristics. It was found that directivity of the RCAs is enhanced when the maximum phase difference in the aperture field remains <90°. TPG superstrates are able to transform the electric field within the RCA cavity to a uniform aperture field above the superstrate, while maintaining the phase variation within ±45°, over a wide range of frequencies, thereby resulting in wideband directivity enhancement.

7. References

1. A. P. Feresidis and J. C. Vardaxoglou, “A broadband high-gain resonant cavity antenna with single feed,” in *European Conference on Antennas and Propagation*, 2006, pp. 1–5.

2. Z. C. Ge, W. X. Zhang, Z. G. Liu, and Y. Y. Gu, “Broadband and high gain printed antennas constructed from Fabry-Perot resonator structure using EBG or FSS cover,” *Microwave and Optical Technology Letters*, **48**, 7, 2006, pp. 1272–1274.

3. S. Muhammad, R. Sauleau, and H. Legay, “Small-size shielded metallic stacked Fabry-Perot cavity antennas with large bandwidth for space applications,” *IEEE Transactions on Antennas and Propagation*, **60**, 2, 2012, pp. 792–802.

4. A. R. Weily, K. P. Esselle, T. S. Bird, and B. C. Sanders, “Dual resonator 1-D EBG antenna with slot array feed for improved radiation bandwidth,” *IET Microwaves, Antennas & Propagation*, **1**, 1, 2007, pp. 198–203.

5. R. M. Hashmi, K. P. Esselle, and S. G. Hay, “Directive beaming with lens-like superstates for low profile Fabry-Perot cavity antennas,” in *International Symposium on Antenna Technologies and Applied Electromagnetics (ANTEM)*, July 2014, pp. 1–2.

6. R. M. Hashmi and K. P. Esselle, “A class of extremely wideband resonant cavity antennas with large directivity-bandwidth products,” IEEE Transactions on Antennas and Propagation, **64**, 2, 2016, pp. 830-835.